Investigating the Effect of Magma Ocean Solidification Rate on Early Atmosphere Formation

Vibha Padmanabhan

November 2, 2021

1 Abstract

The magma ocean stage of terrestrial planets' evolution is closely related to the redox state of their early atmospheres. Previous work has assumed the existence of deep magma oceans which remained molten for timescales comparable to that of planetary accretion. However, the lifetime of a magma ocean is likely orders of magnitude shorter. The deep magma ocean assumption also does not definitively explain the oxidized nature of Earth's early atmosphere and could result in a mantle composition that differs from what is observed. Thus, in this work, we aim to quantify the effects of a rapidly solidifying magma ocean on the atmospheric redox state and on siderophile (iron-loving) element concentrations in the mantle. We do so by constructing a thermochemical model of the mantle and atmosphere of a planetary body under the assumption that its magma ocean solidifies relatively quickly. Testing the rapid solidification model would improve our understanding of the key processes affecting the redox evolution of terrestrial planets.

2 Introduction

The magma ocean stage is a period undergone by terrestrial planets during their evolution. In this stage, the young planet accretes mass through constant collisions from other bodies – impactors – to its surface. A magma ocean (MO) is expected to persist for a time period on the order of 10 kyr. The magma ocean stage has been suggested to be particularly important to determine the redox state of the primitive atmospheres of terrestrial planets: the redox state of the magma ocean is expected to be the redox state of the atmosphere, as volatiles which eventually make up the atmosphere are thought to have been degassed from the magma ocean (Lebrun et al., 2013). The redox state of the magma ocean in turn is governed by equilibria between metals in the metal phase and in the silicate phase, such as those shown below:

$$2\,\mathrm{Fe} + \mathrm{SiO_2} \rightleftharpoons 2\,\mathrm{FeO} + \mathrm{Si} \tag{1}$$

$$2\,\mathrm{Ni} + \mathrm{SiO_2} \rightleftharpoons 2\,\mathrm{NiO} + \mathrm{Si} \tag{2}$$

Using these reactions the redox state of the magma ocean (and thus of the atmosphere) can be determined through calculating the value of oxygen fugacity (fO_2) relative to the iron-wustite (IW) buffer (Hirschmann, 2012).

Namely, the fugacity is given by

$$\ln f\mathrm{O_2} - IW = 2\frac{X_{\mathrm{FeO}}}{X_{\mathrm{Fe}}}, \tag{3}$$

where X_{FeO} and X_{Fe} denote the concentrations of FeO in silicate melt and Fe in the metal phase, respectively. Equilibrium constants (K_d) for these equations were adopted from Rubie et al. (2015) equation 3.

Earlier work has often assumed the existence of deep magma oceans that persist over long timescales, along with the existence of a metal pond. A metal pond is created by the cores of incoming impactors and accumulates at the bottom of the magma ocean. The persistence of a magma ocean over long timescales would allow the metal pond and silicate components in the magma ocean to remain in equilibrium throughout the accretionary phase of the planet. However, the lifetime of a magma ocean is likely short, as mentioned above, and so this assumption may be flawed. The rapid solidification model assumes that magma oceans solidified relatively quickly, and this has two main implications: 1) the equilibration pressure is determined not by the pressure at a depth proportional to the depth of the magma ocean (as it is usually taken to be in the deep magma ocean model) and 2) rapid solidification could result in the formation of a solid layer between the metal pond and silicate, cutting off the metal reservoir (Fe) from the silicate. This drives reactions (4) and (5) to the right, favoring the production of H_2O and CO_2, which are oxidized compounds. Contrast this with the scenario wherein Fe is still present in the system; in this case, the large amount of Fe in the metal pond relative to the other species in the equilibrium would drive the equilibria towards the production of reduced volatiles. We refer to reactions (4) and (5) as the re-equilibrium reactions.

$$2\,\mathrm{FeO} + 2\,\mathrm{H_2} \rightleftharpoons 2\,\mathrm{Fe} + 2\,\mathrm{H_2O} \tag{4}$$

$$\mathrm{FeO} + \mathrm{CO} \rightleftharpoons \mathrm{Fe} + \mathrm{CO_2} \tag{5}$$

To determine equilibrium constants for these reactions, data were taken from the JANAF database and fit using a linear regression. We assumed the activity coefficient of all species to be 1, and thus their chemical potential was equal to their Gibbs free energy of formation.

3 Methods

3.1 Estimation of the Timescale of Solidification of a Magma Ocean

We estimated the timescale of solidification of the magma ocean of an Earth-like planet (see Fig 1), and this amounted to about 4000 years, which is accurate to order of magnitude.

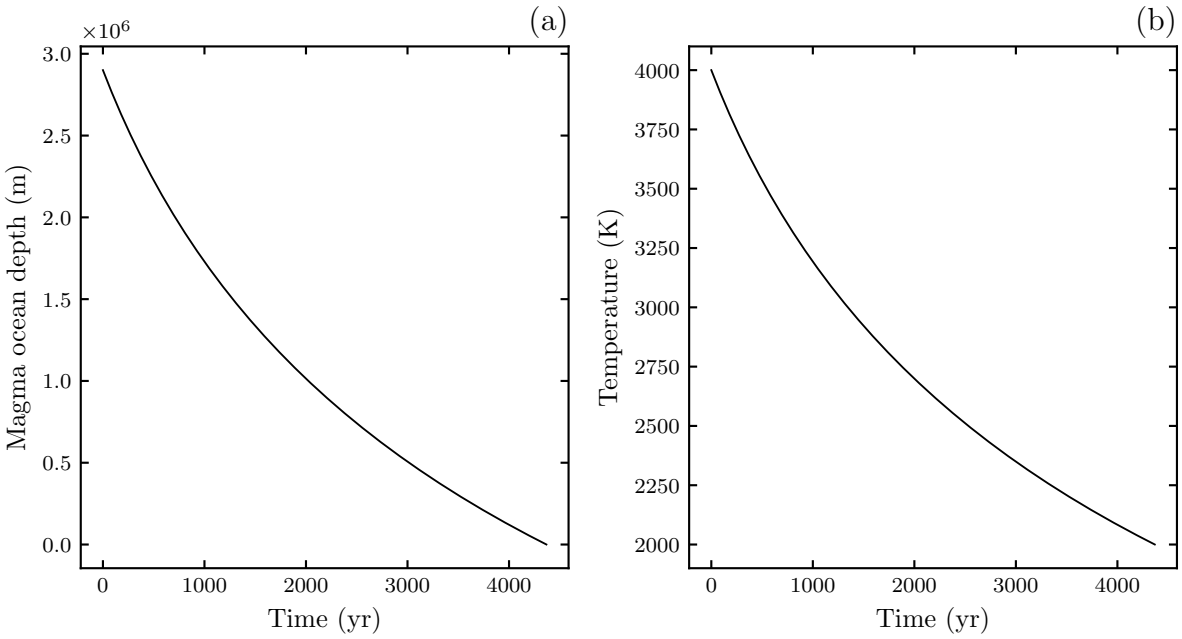

Fig. 1: The the evolution of a magma ocean's depth (a) and its temperature (b)

Using O'Brien et al. (2006), assuming that impacts to a planetesimal occurred at roughly equal intervals over a 100 Myr accretionary period, we determined that the average time between consecutive impacts is about 100 kyr, which our calculations show is an ample amount of time for a magma ocean even as deep as on an Earth-sized planet to solidify.

For all models, we used the compositions resembling CI chondrites for planetesimal and impactor mantles as shown in Table A1, and core as shown in Table A2. The core radius of impactors and initial core radius of the planet in sections 3.3 and 3.4 were calculated assuming core:mantle mass ratio as 1:3.

3.2 Rudimentary Model

We built up to the rapid solidification model in a series of steps. First, a simple model of an impactor with radius 100 km, fully differentiated into core and mantle, colliding with a fully differentiated planetary embryo with radius 1000 km and a magma ocean of 300 km depth was built (i.e., the rudimentary model did not have a deep magma ocean). This was then extended by colliding impactors of different sizes with the planet. We assumed complete equilibration of the impactor's mantle with the magma ocean of the planetary embryo (Wade and Wood, 2005). The relevant equations are (1) and (2). Table 1 shows the parameters of the rudimentary model, including the equilibration temperature, T_{eq}, and the equilibration pressure, P_{eq}. We used approximately an CI-chondritic composition for the initial planetesimal and for impactors. Because we didn't consider all elements in the mantle, the wt% of each element considered was scaled up such that the sum of weight percents of all species totalled 100%.

Parameter	Function
h	$0.3h_m$
P_{eq}	$\rho_m g h$
T_{eq}	$664.48(\frac{P_{eq}}{1.336 \cdot 10^9} + 1)^{\frac{1}{7.437}} + 1189.26(\frac{P_{eq}}{6.594 \cdot 10^9} + 1)^{\frac{1}{5.374}}$

Table 1: Magma ocean depth h is set to 30% of the mantle depth, h_m. Mantle density, ρ_m, and gravitational acceleration g are given in Table A2. The equilibration temperature, T_{eq}, is modelled based on T_{liquidus} and T_{solidus} given in Monteux et al. (2016). Here, $T_{eq} = 0.6\ T_{\text{liquidus}} + 0.4\ T_{\text{solidus}}$.

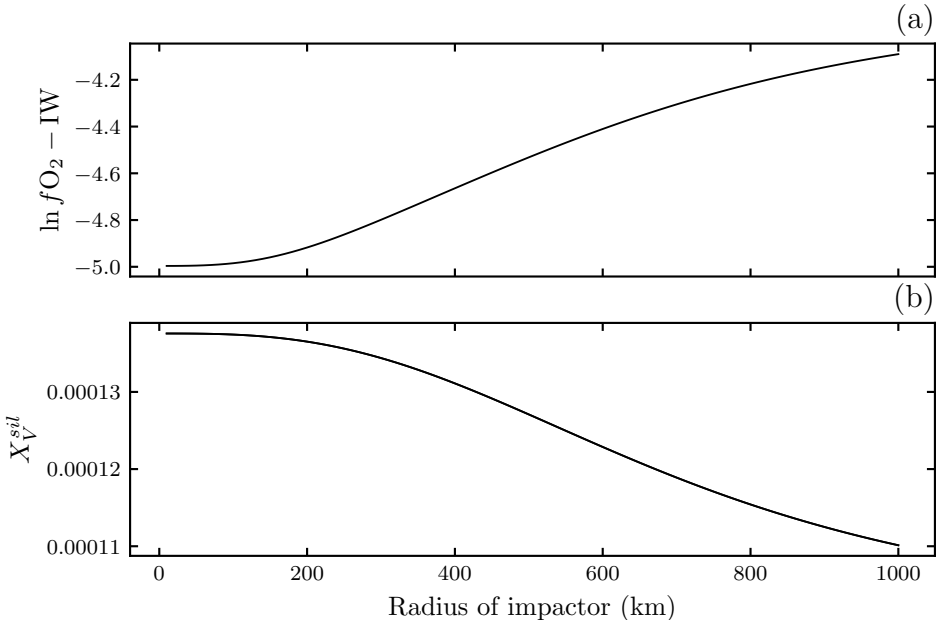

Fig. 2: Plotting (a) the oxygen fugacity of the mantle, $\ln fO_2 - \mathrm{IW}$ and (b) the concentration of V in the mantle for the planetary embryo against impactors of different sizes.

3.3 Deep Magma Ocean Model

Next, a deep magma ocean model was constructed. The purpose of building this model was to determine the value of fO_2 - IW that would result from the deep magma ocean assumption and benchmark our results using Rubie (2015). In this model, a planetesimal with radius 100 km is bombarded by impactors of increasing size until the planetesimal grows to a size of 1000 km in radius. Throughout the evolutionary period, the depth of the magma ocean is 70% the depth of the mantle. After equilibration, the silicate in the magma ocean is mixed with the rest of the mantle such that the mantle becomes compositionally homogeneous after each impact, as in Rubie et al. (2015). This is justified by the highly convective nature of the early Earth's mantle. The equilibrated metal is added to the core of the impactor, and delivered to the solid part of the mantle, such that it does not remain in equilibrium. The parameters of the deep magma ocean model are the same as in Table 1, although the magma ocean depth h is set to $0.7h_m$, rather than $0.3h_m$.

3.3.1 Impactor Size

In the deep magma ocean and rapid solidification models, the impactor radius was set to $\frac{1}{5}r_{planet}$ where r_{planet} denotes the radius of the planet at that time in its evolution. N-body simulations predict that impactor sizes increase over time (O'Brien et al., 2006). Impactor radii of $\frac{1}{3}r_{planet}$ and $\frac{1}{7}r_{planet}$ are also investigated for the deep magma ocean model, but this did not result in a significant change to the final fugacity. Thus, we chose to keep impactor radii equal to $\frac{1}{5}r_{planet}$.

3.3.2 Heterogeneous and Homogeneous Accretion

Homogeneous and heterogeneous accretion are two theories regarding the differentiated nature of the Earth into its core and mantle. In the homogeneous accretion scenario, the material accreted by the planet has a homogeneous composition and the planet undergoes differentiation interally. In the heterogeneous case, the composition of material accreted onto the Earth was heterogeneous, e.g. early material may have been in a reduced state and material towards the end of the accretionary period would have been more oxidized (Righter 2003).

To identify the best fit model, both heterogeneous and homogeneous cases were modelled under the deep magma ocean assumption. Moreover, two cases were considered in the heterogeneous scenario. In the first case, the incoming material was more oxidized earlier on in the accretionary phase and in the second case, it was more reduced earlier on in the accretionary phase. The redox state of the accreted material was controlled by varying the FeO content of the impactors over time. While the second case (accretion of increasingly oxidized material over time) is likelier to occur in nature (Wade and Wood (2005), Wood et al. (2006)), we also included the first case for completeness.

3.3.3 metal pond Lifetime

Because the metal pond is heavier than the underlying solidified mantle, it would be transported to the core by Rayleigh-Taylor instability. We estimated the lifetime of the metal pond in our deep magma ocean model using equation 94 of Mondal and Korenaga (2018). The lifetime of the metal pond is highly sensitive to the viscosity of the mantle, e.g. for every order of magnitude by which the viscosity of the lower mantle increases, the lifetime of the metal pond also increases by an order of magnitude. Fig 3 shows the lifetime of the metal pond over time up till planetary embryo size, taking viscosity of the lower mantle to be 10^{19} Pa s and viscosity of liquid iron to be 10 Pa s. Thus, if the viscosity of the lower mantle is better constrained in the future, and if it is shown to be an order of magnitude (or higher) larger than 10^{19} Pa s, it would be beneficial to model the deep magma ocean model with the presence of a metal pond. This would likely drive the $fO_2 - \text{IW}$ higher, because more Fe would be present, thus generating more FeO by Le Chatelier's principle. Conversely, re-equilibrium could also play an important role in the deep MO, if the metal pond sinks quickly compared to the intervals between impacts. We did not consider these scenario in depth because a deep magma ocean is unlikely to persist.

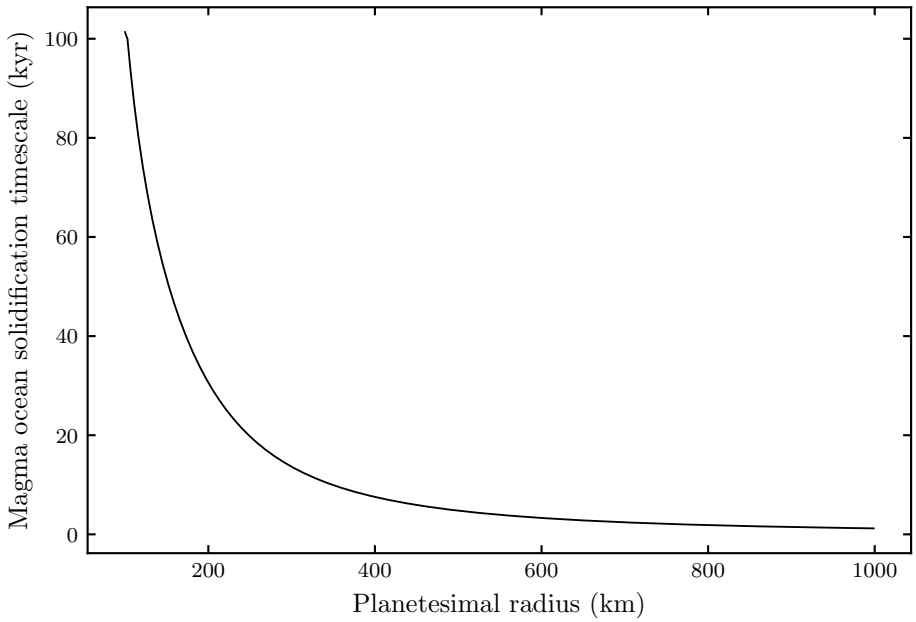

Fig. 3: The timescale of the Rayleigh-Taylor instability for the metal pond throughout the evolutionary period of the planetesimal.

3.4 Rapid Solidification Model

Based on the work of O'Brien et al. (2006), we can infer that on average, the intervals between impacts to the growing Earth were on the order of 90,000 years. Hence, it is plausible that the timescale of

solidification of the magma ocean of a planetesimal is shorter than the intervals between impacts, which consequently implies that each impact would result in the formation of a new magma ocean, which remains molten for long enough for equilibration to occur (on the order of 2 weeks) and solidifies.

In the rapid solidification model, we consider impactors colliding with a planetesimal with a fully solidified surface. Upon each impact, a magma ocean of constant depth is formed all over the surface of the planetesimal and the core of the impactor is considered to equilibrate with the entire magma ocean. The depth of the magma ocean is taken to be directly proportional to the volume of the impactor (Cintala and Grieve, 1998). The same T_{eq} and P_{eq} as in Table 2 are used, h is modelled by the following equation:

$$h = r_p - (r_p^3 - \frac{3}{4\pi} V_{melt})^{\frac{1}{3}}$$

where r_p is the radius of the planet, and $V_{melt} = kV_{impactor}$ where $V_{impactor}$ denotes the volume of the impactor. The different values of k tested were 10, 50 and 100.

After modelling the equilibria described by equations (1) and (2) we considered re-equilibrium of FeO with CO and H_2O, which are described by equations (4) and (5). Under the deep magma ocean assumption, equations (4) and (5) would favor the production of H_2 and FeO, because Fe remains in contact with the volatiles in the magma ocean. However, if we consider the removal of Fe from the system, the equilibria will be driven towards producing oxidized volatiles.

As the amount of H_2 and C in the mantle isn't well-constrained (Hirschmann and Dasgupta, 2009), we considered all C and H in the planet and impactor mantles to be present in the form of CO_2 and H_2O, with weight percents of C and H given in Table A1, and solved for $\frac{H_2O}{H_2}$ and $\frac{CO_2}{CO}$ ratios using fO_2.

4 Results

The results of the heterogeneous and homogeneous accretion models under the deep magma ocean assumption are shown in Table 2. The model that agreed best with our benchmark final compositions (Rubie et al., 2015) was the homogeneous accretion scenario, and thus we also assumed homogeneous accretion for the rapid solidification model. The final FeO content and Si content in the deep magma ocean model was very sensitive to the FeO content set in the initial conditions. The most oxidized final fO_2 - IW under the deep magma ocean assumption was -4.00, which is still strongly reduced. The fugacity values for the different models tested are tabled in Table 3.

Species	Homogeneous accretion	Het. accretion (increasing FeO)	Het. accretion (decreasing FeO)
Fe_m	79.2	67.5	75.3
Si_m	4.79	0.38	6.11
Ni_m	15.7	32.8	16.2
V_m	42.8 ppm	8.6 ppm	52.6
Fe_{sil}	13.0	28.7	11.4
Si_{sil}	39.9	25.3	41.9
Ni_{sil}	18.9	32.8	20.0
V_{sil}	271 ppm	247 ppm	290 ppm

Table 2: Final compositions of core and mantle for a planetary embryo-sized body. All units are wt% unless otherwise specified. A subscript m denotes the amount of the species in the core, and the subscript *sil* denotes the amount of the species in the magma ocean (in silicate phase, the reported wt% are those of the oxides of the metal).

The rapid solidification model performed poorly without incorporation of the re-equilibrium process, i.e. the final fugacity in the rapid equilibrium model where re-equilibrium did not occur was lower than

Model	Melt factor	$\ln fO_2$ - IW
Deep magma ocean	NA	-4.00
Rapid solidification	10	-4.10
Rapid solidification	50	-4.08
Rapid solidification	100	-4.04

Table 3: Comparing the final values of $\ln fO_2$ - IW for a planetary embryo-sized body for the deep magma ocean model and the models under the rapid solidification assumption. A more negative fugacity value indicates a more reduced atmosphere.

the fugacity of the deep magma ocean model.

After having incorporated re-equilibrium, the atmosphere was found to be enriched in H_2O and CO_2, which are oxidized compounds. Fig 4 plots the $\frac{H_2O}{H_2}$ ratio in the atmosphere, comparing the cases with and without re-equilibrium under the rapid solidification assumption. It is clear that incorporating the re-equilibrium processes drove the amounts of oxidized volatiles in the atmosphere up by about an order of magnitude, as compared to the model wherein re-equilibrium was not considered.

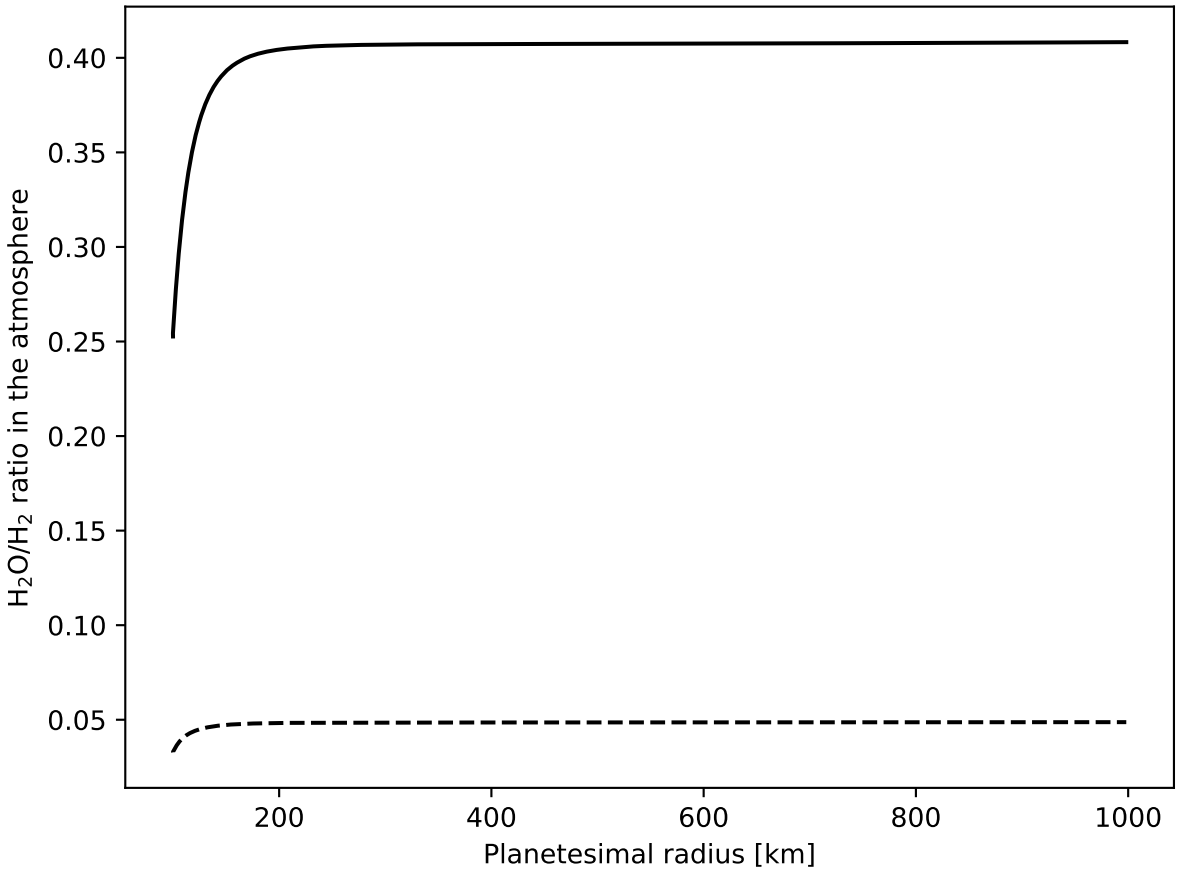

Fig. 4: Oxidized vs reduced compound ratio in the deep magma ocean (dashed) vs re-equilibrium (solid).

The size of the impactors and the melt factor (for the rapid solidification model) did not seem to significantly (by an order of magnitude or more) affect the final fO_2 in either model.

5 Discussion

The rapid solidification model seemed to perform similarly to the deep MO model when re-equilibrium was not considered, though the final fugacity in the deep magma ocean model corresponded to a slightly more oxidized atmosphere. There are two reasons this could be the case; one, the amount of silicate melt with which the impactor core equilibrates is higher in the deep magma ocean case, and two, the equilibrium pressure is higher in the deep magma ocean case. To isolate which factor is more important, the deep magma ocean model was run with P_{eq} = CMB pressure with $h = 70\%$ of the depth of the mantle and then with P_{eq} = CMB pressure with $h = 100\%$ the depth of the mantle. The results showed that pressure plays a more important role than the amount of material equilibrating.

Re-equilibrium seems to be important to obtain an atmosphere enriched in oxidized volatiles. Thus, this is a scenario worth considering further; consideration of the equilibria between other metal oxides and volatiles in the magma ocean would provide more precise results on the ratio of oxidized to reduced compounds in the primitive atmosphere.

6 Conclusion

We modelled and compared a deep magma ocean with the alternative theory of a rapidly solidifying magma ocean. If one considers the presence of a metal pond in the deep magma ocean model, it seems likely that the reaction between metal and volatiles in the magma ocean will enrich the atmosphere with reduced compounds, which is what we confirmed with our deep magma ocean model. The rapid solidification theory seems to be promising in terms of the enrichment of the atmosphere-magma ocean system with oxidized compounds through re-equilibrium (the reaction of metal oxides with volatiles in the magma ocean). Re-equilibrium in the rapid solidification case produces oxidized compounds in the magma ocean-atmosphere system because the metal reservoir is cut off from the system. Further work should be done to explore whether the species we considered during re-equilibrium (CH_4, CO_2, H_2O) existed under the pressure, temperature and chemical conditions of a magma ocean environment, or whether the elements carbon and hydrogen were in different oxidation states than we assumed. Additionally, a more detailed interior model would strengthen our results, since our pressure model $\rho_m g h$ underestimated pressures, especially in the deep magma ocean model: e.g., the CMB pressure for the Earth was estimated to be about 98 GPa whereas in reality it is 136 GPa. It would also be useful to add the elements to the mantle which we have excluded, such that a scaling factor is unneeded.

A Appendix

Modelling of g: We use a power law $g \propto M_p^{0.503}$, where M_p denotes mass of the planet. The proportionality constant k is solved for using Mars' mass to gravitational acceleration ratio.

B Acknowledgments

I would like to thank my mentor Dr. Yoshinori Miyazaki for his support and guidance throughout the project, and Samuel P. and Frances Krown for supporting my SURF through their generous donations.

Parameter	Amount (wt%)	Source
Fe	6.22	Lyubetskaya and Korenaga (2007)
Ni	0.00	Lyubetskaya and Korenaga (2007)
V	6.06×10^{-3}	Rubie et al. (2015)
Si	21.09	Lyubetskaya and Korenaga (2007)
Mg	23.41	Lyubetskaya and Korenaga (2007)
H	0.01	Hirschmann and Dasgupta (2009)
C	0.01	Hirschmann and Dasgupta (2009)

Table A1: Bulk starting composition of impactor and planetesimal mantles. Based on CI-chondritic relative abundances from Rubie et al. (2015). Water and carbon dioxide abundances are based on Hirschmann and Dasgupta (2009), which suggests that the H / C ratio of the bulk Earth is 1.

Parameter	Value (kg m^{-3})
Mantle density ρ_m	3000
Core density ρ_c	8000

Table A2: Core and mantle densities for bodies.

References

Cintala, M. J. and Grieve, R. A. F. (1998). Scaling impact melting and crater dimensions: Implications for the lunar cratering record. *Meteoritics and Planetary Science*, 33:889–912.

Hirschmann, M. M. (2012). Magma ocean influence on early atmosphere mass and composition. *Earth and Planetary Science Letters*, 341:48–57.

Hirschmann, M. M. and Dasgupta, R. (2009). The H/C ratios of Earth's near-surface and deep reservoirs, and consequences for deep Earth volatile cycles. *Chemical Geology*, 262:4–16.

Lebrun, T., Massol, H., Chassefiere, E., Davaille, A., Marcq, E., Sarda, P., Leblanc, A., and Brandeis, G. (2013). Thermal evolution of an early magma ocean in interaction with the atmosphere. *Journal of Geophysical Research: Planets*, 118:1155–1176.

Lyubetskaya, T. and Korenaga, J. (2007). Chemical composition of Earth's primitive mantle and its variance. *Journal of Geophysical Research*, 112.

Mondal, P. and Korenaga, J. (2018). The Rayleigh–Taylor instability in a self-gravitating two-layer viscous sphere. *Geophysical Journal International*, 212:1859–1867.

Monteux, J., Andrault, D., and Samuel, H. (2016). On the cooling of a deep terrestrial magma ocean. *Earth and Planetary Science Letters*, 448:140–149.

O'Brien, D. P., Morbidelli, A., and Levison, H. F. (2006). Terrestrial planet formation with strong dynamical friction. *Icarus*, 184:39–58.

Rubie, D. C., Jacobson, S. A., Morbidelli, A., O'Brien, D. P., Young, E. D., de Vries, J., Nimmo, F., Palme, H., and Frost, D. J. (2015). Accretion and differentiation of the terrestrial planets with implications for the compositions of early-formed solar system bodies and accretion of water. *Icarus*, 248:89–108.

Wade, J. and Wood, B. J. (2005). Core formation and the oxidation state of the Earth. *Earth and Planetary Science Letters*, 236:78–95.

Wood, B. J., Walter, M. J., and Wade, J. (2006). Accretion of the Earth and segregation of its core. *Nature*, 441:825–833.